

Quantitative Measurement of Renal Perfusion Following Transplant Surgery

James L. Lear, Ulrich Raff, Ravi Jain, and J. Gerard Horgan

Division of Nuclear Medicine, University of Colorado Health Sciences Center, Denver, Colorado

We developed an easily implemented clinical procedure for quantitative perfusion measurements in transplanted kidneys using intravenously administered [^{99m}Tc]DTPA and the tracer fractionation technique. $F = A_k(T) / \int_0^T [A_a(t)/V_a] dt$, where F = renal blood flow, $A_k(T)$ = DTPA activity in kidney at time = T , V_a = ultrasonographically measured femoral artery segment volume, T = time postinjection of F determination, and $A_a(t)$ = time course of DTPA activity in femoral artery segment. The technique was applied to a group of 80 studies in 35 patients in whom an independent clinical determination of transplant function was available. Blood flow (units of ml/min) measured 439 ± 83 in normally functioning transplants, 248 ± 63 in transplants with acute tubular necrosis, 128 ± 62 in transplants with rejection, and 284 ± 97 in transplants with cyclosporine toxicity. These preliminary results indicate potential usefulness of this method in the evaluation of renal function following transplant surgery.

J Nucl Med 29:1656-1661, 1988

Quantitative techniques for evaluation of renal transplant functional parameters such as effective renal plasma flow (ERPF) and glomerular filtration rate (GFR) have been developed (1-17). In addition, empirical methods to evaluate relative blood flow or perfusion in transplants have been proposed (18-23). No quantitative method for the scintigraphic evaluation of renal transplant perfusion, however, has been developed to the point of routine application. Because perfusion is significantly impaired by post-transplant diseases such as rejection, a method for its quantitative measurement could have important clinical applicability.

Recently, a model has been described which permits the determination of organ perfusion using external detectors and first-pass data (24). This flow model has been applied to myocardial perfusion (25) and has been suggested as an approach to the determination of renal perfusion (26-27). We further developed this model and applied it to measurement of blood flow in renal transplants.

MATERIALS AND METHODS

The technique developed for measuring renal blood flow in this study was derived from previously described and vali-

dated first-pass tracer fractionation methods (24,28,29). These models are based on the fact that during the initial pass of a tracer through an organ, there exists a time before the tracer reaches the venous drainage, when all the tracer is within the organ of interest (Fig. 1A). Using this premise, blood flow to the organ can be calculated using the following relationship:

$$F = A_k(T) / \int_0^T C_a(t) dt, \quad (1)$$

where

- F = blood flow to the organ,
- $A_k(T)$ = organ tracer activity at time, T
- $C_a(t)$ = concentration of tracer in the arterial blood entering the organ as a function of time.

In previous applications of this model, $C_a(t)$ has been determined by arterial blood sampling (28) or by the use of positron emission tomography (25). It has also been suggested that $C_a(t)$ can be estimated by measuring total activity in a region of interest over the aorta using a gamma camera and assuming that the volume of the vascular region of interest is the same for all patients (26,27).

We modified the above techniques by scintigraphically measuring activity in an arterial region of interest, the proximal femoral artery, and determining its volume using ultrasound. The femoral artery was chosen because its geometry can be defined using real time ultrasound, it can be placed within the same field of view as a transplanted kidney, and its activity profile is temporally similar to that of the transplanted renal artery.

$$C_a(t) = A_a(t)/V_a, \quad (2)$$

Received Dec. 21, 1987; revision accepted May 19, 1988.

For reprints contact: James L. Lear, MD, Nuclear Medicine (A034), University of Colorado Health Sciences Center, 4200 E. 9th Ave., Denver, CO 80262.

where

$A_a(t)$ = time course of arterial activity of tracer

V_a = ultrasonically determined volume of arterial region

thus

$$F = A_k(T) / \int_0^T C_a(t) dt, \quad (3)$$

The model was implemented as part of routine diethylene-triaminepentaacetic acid (DTPA) renal scanning. Patients were positioned so that the renal transplant and femoral arteries were within the field of view of a square, large field-of-view gamma camera (model SX-300, Picker International, Inc., Cleveland, OH) and given bolus intravenous injections of 10–15 mCi of technetium-99m (^{99m}Tc) DTPA. Data was acquired during 30 sec at the rate of two frames per second and digitized into matrices of 64×64 pixels using a dedicated nuclear medicine computer (PCS-512 Picker International, Inc., Cleveland, OH). Regions of interest were drawn around the renal transplant and segments of ipsilateral and contralateral proximal femoral arteries (Fig. 1B). The arterial regions were drawn so that they were 7 pixels in length along the axis of the artery and extended 1 pixel beyond each edge of the artery. The length of the arterial segments were determined multiplying the pixel size (as determined with a precisely machined 20.0 cm phantom) by the number of pixels. Background regions of interest were also evaluated to determine the effects of scatter. The time course of activity in each region was determined. In addition, the time course of activity within the camera's entire field of view was measured to evaluate the significance of potential deadtime count rate loss. Realtime ultrasound was used to determine the mean diameter and hence the volume of the arterial regions of interest.

After correcting the values of $C_a(t)$ and $A_k(T)$ for background, Eq. (3) was applied to the scan and ultrasound data and used to determine renal blood flow. The model expressed in Eq. (3) is valid for all times until initial venous effluent of tracer occurs and therefore the same value of flow should be found at any point in time between bolus arrival and effluent of tracer. This hypothesis was tested by generating graphs of the calculated value of flow as a function of time. Also, because the bolus tended to arrive in the arterial region of interest slightly later than the kidney region of interest, the arterial and renal curves were aligned to the same bolus arrival time. In order to investigate the significance of the accuracy of curve alignment, flow vs. time curves were also generated for conditions where the arterial activity curve was shifted by one second increments earlier and later.

A kidney shaped distensible phantom was used to measure the effects of self-attenuation of activity. Various volumes of water ranging from 250 to 500 ml containing ^{99m}Tc were placed in the phantom. Activity was measured over the phantom and over a plastic syringe containing the same amount of ^{99m}Tc .

The technique was applied to a series of 80 consecutive studies in 35 patients in whom an independent clinical determination of transplant function was available. The patients were clinically divided into four groups based upon parameters including time course of creatinine levels, urinary output, temperature, cyclosporine levels, response to drug therapy, hippuran clearance, time postsurgery, ultrasound tissue ap-

pearance, and Doppler measurements. The four groups were: (a) normally functioning transplant, (b) transplant with post surgical acute tubular necrosis (ATN), (c) transplant with rejection; (d) transplant with cyclosporine toxicity. Patients in whom a clinical diagnosis was ambiguous or in whom the transplant had evidence of infarcts were excluded from the study.

RESULTS

The mean diameter of the proximal femoral arteries ranged from 0.6 cm to 1.4 cm with a mean value of

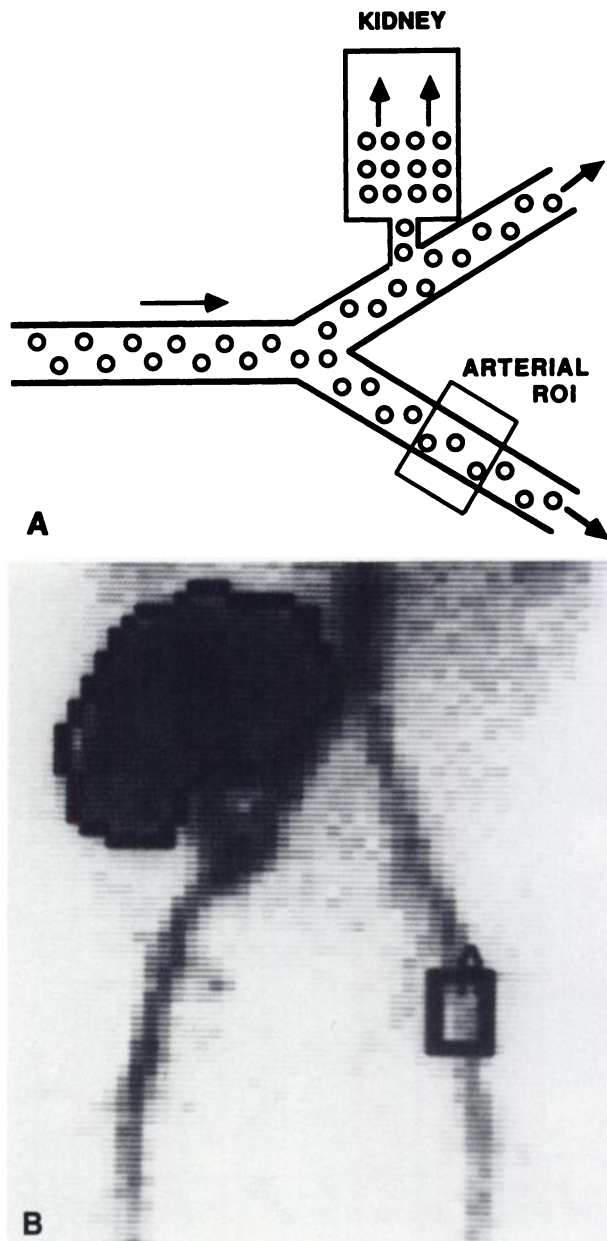


FIGURE 1

A: The basis for the first-pass tracer fractionation model is illustrated. A period of time exists when all of the activity (circles) which has entered an organ remains within the organ. B: Regions of interest are drawn over kidney and contralateral proximal femoral artery for analysis. The contralateral artery is used to minimize the effects of scatter.

1.05 cm in the patients studied. Thus the arterial volumes had a sixfold range ($1.4^2/0.6^2$) across all patients and a two to threefold range compared to the mean value.

Figure 2 contains a typical set of activity curves for the arterial and kidney regions of interest. In all patients, the arterial activity curves rose rapidly to a peak, usually within 4–6 sec, and then rapidly declined as the bolus passed. The rates of rise of the renal activity curves were more varied and the curves tended to peak more slowly and then slowly decline. Activity within the camera's entire field of view remained $<20,000$ counts per second at any time, so deadtime losses were not significant.

When the arterial and renal curves were properly aligned, i.e., bolus arrival times were superimposed, the flow vs. time curve rose rapidly to a plateau representing actual renal flow (Fig. 3). This plateau persisted for ~4–8 sec representing the time during which the tracer had not passed through the kidney to the venous effluent and for which Eq. (3) was therefore valid. The value of flow then decreased as the tracer began to leave the kidney region of interest. Flow versus time curves in which the arterial activity profiles were shifted to a later time than those of the kidney began high and then rapidly decreased to values near actual flow. Flow versus time curves in which the arterial activity profiles were shifted to an earlier time than those of the kidney began low and rose to values near actual flow. The final value of flow used in the clinical analysis was fixed as the value obtained from Eq. (3) for properly aligned curves

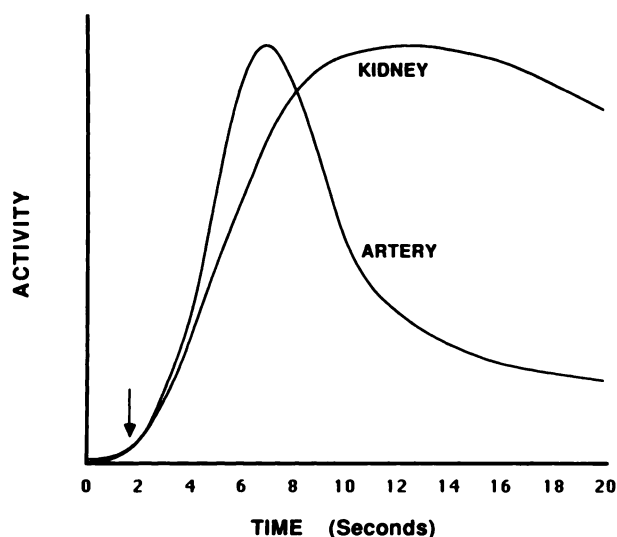


FIGURE 2
Activity versus time relationships for the femoral artery and kidney are shown. Slight differences in bolus arrival times can cause differences in relative positions of the curves. Both curves have been aligned to the same bolus arrival time (arrow) and scaled so that their maximums are at the upper limits of the graph.

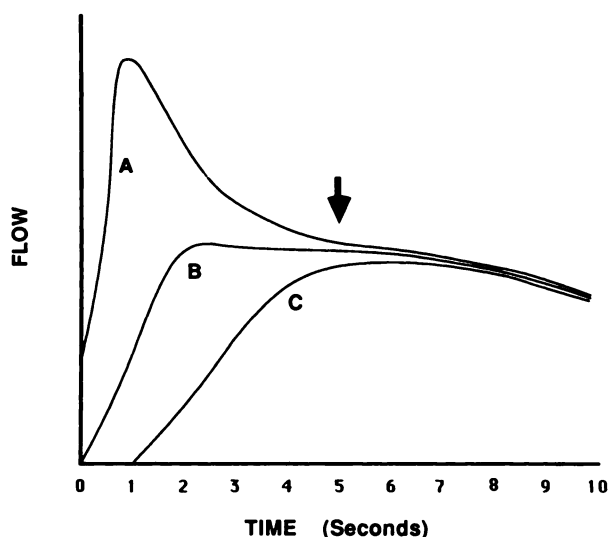


FIGURE 3
A family of flow curves is presented for 1-sec shifts in relative position of the artery and kidney activity curves. When the artery and kidney curves are properly aligned to bolus arrival time, the curve representing flow rapidly reaches the correct value, plateaus for 4–8 sec, and then decreases slowly as the bolus passes through the kidney (B). When the arterial curve is shifted so that the arterial activity arrives later than that of the kidney, the flow curve begins high, then drops to approach the correct flow value, and finally decreases as the bolus passes through the kidney (A). When the arterial is shifted so that it begins before that of the kidney, the flow curve begins low, rises to approach the correct value, and then decreases (C).

at peak bolus activity in the arterial region or 5 sec post bolus arrival time, whichever was earlier.

The time course of activity in background regions of interest indicated that scatter from the kidney could influence activity measured in ipsilateral arterial regions of interest. When contralateral regions were used, scatter contribution dropped to $<5\%$ of activity in the arterial regions of interest up to the bolus peak.

The phantom studies indicated that self-attenuation could range from 8%–17%, depending on the size of the “kidney”. A value of 10% was used to correct the renal activity in the regions of interest.

Considerable differences in renal blood flow were found between the four groups of renal transplant patients. Blood flow measured 439 (mean) ± 83 (s.d.) ml/min in normal functioning transplants, 248 ± 63 ml/min in transplants with postsurgical ATN, 128 ± 72 ml/min in transplants with rejection, and 284 ± 97 ml/min in transplants with cyclosporine toxicity (Fig. 4). The differences between normal, ATN, and rejection were significant ($p < 0.05$). Blood flow in cyclosporine toxicity was significantly different than normal or rejection, but not significantly different than ATN. Normal patients showed little overlap in renal flow values with those suffering from ATN or rejection. Patients with

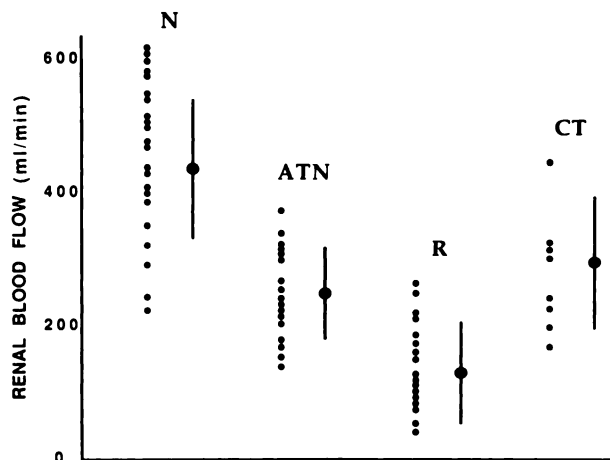


FIGURE 4
Values of renal flow for the four clinical conditions evaluated in this study. Small dots represent individual patient values. Larger dots and line segments represent the mean value and standard deviation for each condition; N = normally functioning transplant, ATN = transplant with acute tubular necrosis, R = transplant with rejection, and CT = transplant with cyclosporine toxicity.

ATN and rejection, however, showed considerable overlap in values with each other. Patients with isolated cyclosporine toxicity were few, and renal flow values showed considerable spread.

DISCUSSION

Model and Methodology

The use of ultrasonically measured arterial volume was found to be important. The sixfold range of values found in this study, as well as the two–threefold range compared to mean volume, indicate that the assumption of a single value for all patients could introduce significant error in flow determination. For any given patient, however, the arterial diameter probably would not change much from study to study, and thus $A_k(T)/\int_0^T A_a(t) dt$ ratio could be used as an index of relative perfusion over time.

The size of the arterial region of interest was chosen as a compromise between requirements of the model and noise in data measurement. The model requires that $C_a(t)$, the concentration of tracer in the arterial blood entering the organ, be known. This concentration is actually the tracer activity, $A_a(t)$, in an infinitesimal volume of blood as it crosses the boundary of the kidney, divided by the infinitesimal volume, V_a . We found, however, that when very tiny arterial ROIs were used, noise in the count measurements was large. On the other hand, when very large regions were used to reduce noise, measured values of $C_a(t)$ would be inaccurate because of smearing of the concentration profiles (30). By using ~3-cm-long arterial regions, noise was

reduced to low levels while permitting accurate estimation of the true arterial input function.

Using the technique developed in this study, normally functioning transplanted kidneys had flow values near 450 ml/min. This value is in close agreement with values of normal native kidney flow, ~500–550 ml/min (31). The somewhat lower values in our study could be caused by some of the assumptions in our model. We used a low value of self-attenuation to correct the measured renal activity. If particular kidneys were larger than the smallest phantom size, true renal activity, and hence flow, could be underestimated. Rather than attempting to measure exact renal and artery depth for each patient, a procedure which would have greatly increased the complexity of the ultrasound examination, we assumed that both the transplanted kidney and femoral artery were the same distance from the skin surface. If the transplanted kidney were actually deeper, its activity, and thus flow, might be slightly underestimated. Finally, we assumed that no venous effluent of activity occurred up to the point of measurement of flow. It is possible that a small amount of tracer could have passed through the kidney within the upper limit of 5 sec used in this study.

A potential source of overestimation of flow occurred in some patients. Occasionally the kidney would be very close to the ipsilateral femoral artery, or even partially overlie it. Kidney regions of interest were drawn in attempts to avoid including such arterial activity, but it is possible that in some instances, overestimation of renal activity might have occurred. Such overestimation in renal activity would also cause overestimation of renal blood flow.

The time point used for the actual flow measurement, the earlier of arterial peak time or 5 sec post bolus arrival time, was based on analysis of the flow versus time curves. The simulations in which the arterial and kidney curves were intentionally misaligned showed that misalignment could introduce errors in flow values. These errors were greatest at early times and decreased with time to insignificance. Such errors were <10% by 5 sec. At later times, errors of underestimation of flow were introduced because of venous effluent of tracer. Thus, the time used in this study was chosen as a compromise between these effects.

Clinical Utility

The first-pass tracer fractionation technique has been validated previously, both generally (24) and in the determination of myocardial perfusion (25). Requirements for successful implementation include the ability to define the activity in the organ of interest and to determine the time course of concentration of activity in an artery with the same blood source as the organ. Both of these requirements were achieved in the measurement of renal flow in this study. The fact that values obtained in normal kidneys were close to values of

normal native renal blood flow supports the validity of the technique.

Acute tubular necrosis caused significant decreases in flow. These decreases, which averaged almost 50%, have not been appreciated previously (16). Rejection tended to cause an even greater decrease in flow, although considerable overlap between ATN and rejection flow values occurred. This overlap would prevent blood flow alone from being used to separate these two pathologies. Fortunately, in clinical practice, ATN and rejection are usually distinguishable by time course and hippuran clearance differences.

A more important diagnostic problem is the ability to separate rejection from cyclosporine toxicity. Our data with respect to blood flow in cyclosporine toxicity was limited to only eight patients and was variable within that group, but the preliminary results did show that flow values with cyclosporine toxicity tended to be higher than those of rejection.

Thus, this preliminary data suggests that measurement of renal transplant perfusion using the first-pass tracer fractionation technique may be clinically useful. Along with determinations of GFR and ERPF, perfusion measurements could help evaluate the functional status of transplanted kidneys and assist in differential diagnosis. The technique requires no additional administration of activity in a patient undergoing a DTPA renal scan and the ultrasound measurement can be performed rapidly. Alternatively, when ultrasound cannot be performed, the ratio of $A_k(T)/\int_0^T A_a(t) dt$ could be used to follow the relative renal perfusion over time in a given patient.

ACKNOWLEDGMENTS

This work was supported in part by a University of Colorado Academic Enrichment Grant.

REFERENCES

1. Sapirstein LA, Vidt DG, Mandel MJ, Hanusek G. Volumes of distribution and clearances of intravenously injected creatinine in the dog. *Am J Physiol* 1955; 181:330-336.
2. Taplin GV, Dore EK, Johnson DE. The quantitative radiorenogram for total and differential renal blood flow measurements. *J Nucl Med* 1963; 4:404-409.
3. Blaufox MD. Compartmental analysis of the radiorenogram and kinetics of 131-I-hippuran. *Prog Nucl Med* 1972; 2:107-214.
4. DeGrazia JA, Scheibe PO, Jackson PE, et al. Clinical applications of a kinetic model of hippurate distribution and renal clearance. *J Nucl Med* 1974; 15:102-114.
5. Chisohlm GD, Short MD, Glass HI. The measurement of individual renal plasma flows using 123-I-hippuran and the gamma camera. *Br J Urol* 1974; 46:591-600.
6. Dubovsky EV, Logic GR, Rietheim AG. Comprehensive evaluation of renal function in the transplanted kidney. *J Nucl Med* 1975; 16:1115-1120.
7. Schlegel JU, Hamway SA. Individual renal plasma flow determination in two minutes. *J Urol* 1976; 116:282-285.
8. Zielinski FW, Holly FE, Robinson GD, Bennett LR. Total and individual kidney function assessment with iodine 123 orthoiodohippurate. *Radiology* 1977; 125:753-759.
9. Pors-Nielsen S, Lehd-Moller M, Trap-Jensen J. ^{99m}Tc DTPA scintillation camera renography: a new method for estimation of single kidney function. *J Nucl Med* 1977; 18:112-117.
10. Piepsz A, Dobbeleir A, Erbsman F. Measurement of separate kidney clearance by means of ^{99m}Tc DTPA complex and a scintillation camera. *Eur J Nucl Med* 1977; 2:173-177.
11. Tamminen TE, Riihimaki EG, Tahti EE. A gamma camera method for quantitation of split renal function in children followed for viscoureteric reflux. *Pediatric Radiol* 1978; 7:78-84.
12. Stadalnik RC, Vogel JM, Jansholt AL, et al. Renal clearance and extraction parameters of ortho-iodohippurate (I-123) compared with OIH (I-131) and PAH. *J Nucl Med* 1980; 21:168-170.
13. Diethilm AG, Dubovsky EV, Whelchel JD, et al. Diagnosis of impaired renal function after kidney transplantation using renal scintigraphy, renal plasma flow, and urinary excretion of hippurate. *Ann Surg* 1980; 191:604-616.
14. Tauxe WN, Dubovsky EV, Kidd T, et al. New formulae for the calculation of effective renal plasma flow. *Eur J Nucl Med* 1982; 7:51-54.
15. Gates GF. Glomerular filtration rate: estimation from fractional renal accumulation of ^{99m}Tc DTPA (stanous). *Am J Roentgenol* 1982; 183:565-570.
16. Kirchner PT, Rosenthal L. Renal transplant evaluation. *Semin Nucl Med* 1982; 12:370-378.
17. Dubovsky EV, Russell CE. Quantitation of renal function with glomerular and tubular agents. *Semin Nucl Med* 1982; 12:308-329.
18. Rosenthal L. Radiotechnecium renography and serial imaging for screening renovascular hypertension. *Semin Nucl Med* 1974; 4:97-116.
19. Rosenthal L, Mangel R, Lisbona R, Lacourciere Y. Diagnostic applications of radiopertechetate and radiohippurate imaging in post-renal transplant complications. *Radiology* 1974; 111:347-358.
20. Hilson AW, Maisey MN, Brown CB, et al. Dynamic renal transplant imaging with ^{99m}Tc DTPA (sn) supplemented by a transplant perfusion index in the management of renal transplants. *J Nucl Med* 1978; 19:994-1000.
21. Clorius JH, Dreikorn K, Zelt J, et al. Renal graft evaluation with pertechetate and I131-hippuran. *J Nucl Med* 1979; 20:1029-1037.
22. Ford K, Harris CC, Coleman RE, Dunnick NR. The radionuclide renogram as a predictor of relative renal blood flow. *Radiology* 1983; 149:819-821
23. Anaise D, Oster ZH, Atkins HL, et al. Cortex perfusion index: a sensitive detector of acute rejection crisis in transplanted kidneys. *J Nucl Med* 1986; 27:1697-1701.
24. Mullani NA, Gould KL. First-pass measurements of regional blood flow with external detectors. *J Nucl Med* 1983; 24:577-581.
25. Mullani NA, Goldstein RA, Gould KL, et al. Myocar-

- dial perfusion with rubidium-82. I. Measurement of extraction fraction and flow with external detectors. *J Nucl Med* 1983; 24:898-906.
26. Graham MM, Vea HW, Schwartz AN. Tissue blood flow from bolus first-pass data applied to renal transplants and the penis [Abstract]. *J Nucl Med* 1987; 28:406.
 27. Arnold JM, Arnold J, Arnold JS. Renal blood flow in ml/min by first pass analysis using aorta as supply conduit [Abstract]. *J Nucl Med* 1987; 28:405-406.
 28. Sapirstein LA. Fractionation of the cardiac output of rates with isotopic potassium. *Circ Res* 1956; 4:689-692.
 29. Peters AM, Myers MJ, Hartnell G, et al. Non-invasive measurement of renal blood flow (RBF) with DTPA [Abstract]. *J Nucl Med* 1987; 28:646.
 30. Klingensmith WC. Evaluation of a physiologic method of interpreting first circulation time indicator curves. *Invest Radiol* 1986; 21:566-570.
 31. Guyton AC. In: Basic human physiology: normal function and mechanisms of disease. Philadelphia: W.B. Saunders Co., 2nd Ed., 1977